Chapter 5
Electric Propulsion

5.1 Overview

Electric propulsion engines differ from thermal engines in that, among other things, the propellant does not serve as an energy source to heat and accelerate the propellant mass in the combustion chamber. Rather acceleration is achieved by accelerating ions in an electric field, the energy of which needs to be provided externally by an electric current source. This is both an advantage and a disadvantage at the same time. The advantage is that, theoretically, any amount of energy can be applied to the propellant mass which would in principle permit unlimited exhaust speeds, hence unlimited specific impulse, and therefore unlimited efficiency of the engine. The disadvantage is that the structural mass of the rocket stage increases due to the additional mass of the electric generator, which directly trades with payload mass. Massive generators are required especially for high-I_{sp} engines, so their additional mass may outweigh propellant savings. Therefore, comparisons between different propulsion systems always need to consider the total propulsion system mass: propulsion system, consumed propellant, plus energy supply system.

Another disadvantage of electric propulsion is that ions repel each other, permitting only very low particle densities in the engine chamber, which in turn leads to mass flow densities many orders of magnitude lower than those of chemical engines. This results in very small thrusts. For this reason electric propulsions will not replace launch thrusters in the long run, as thrust is a key figure for launch. This is apart from the problem that their exit pressure is much lower than ambient pressure, which by itself rules out their employment for launch. On the other hand, once outer space has been reached, and especially with interplanetary flights with long flight times, continuous operation with a highly effective ion or Hall-effect thruster often pays off in comparison with a two-impulse transfer with low-efficient chemical propulsions. This is shown in Table 5.1 with the example of a Mars mission.

U. Walter, *Astronautics*, https://doi.org/10.1007/978-3-319-74373-8_5

Table 5.1 Comparison of all-chemical and ion-solar engines for the example of a Mars mission

Parameter	Spacecraft description	
	All-chemical voyager (190 days transit)	Ion-solar voyager (190 days transit)
Injected weight (not including launch vehicle)	3530 kg	4350 kg
Power level	All chemical	23 kW
Approach velocity	4.3 km s^{-1}	1.8 km s^{-1}
Weight at approach	2400 kg	2330 kg
Weight in orbit (excluding retro insert weight)	840 kg	1630 kg
Orbit spacecraft fraction	0.35	0.70
Lander weight	1040 kg	1040 kg
Scientific payload	210 kg	810 kg
Percent scientific payload weight at approach	8.9%	34.9%

5.2 Ion Thruster

Let us have a closer look at ion propulsion as it becomes more and more of practical importance. It is based on the acceleration of cold plasma in a high electric field (see Fig. 5.1). The inflowing propellant atoms are ionized in a relatively voluminous reaction chamber by hitting them with circulating electrons, which knock outer-shell electrons out off the atoms. "Cold" here means that, during the ionization process no internal states of the atom are excited. This is achieved by using noble gas atoms, which occur only as single atoms and hence quite naturally lack any rotational or vibrational modes to be excited. These singly charged ions then

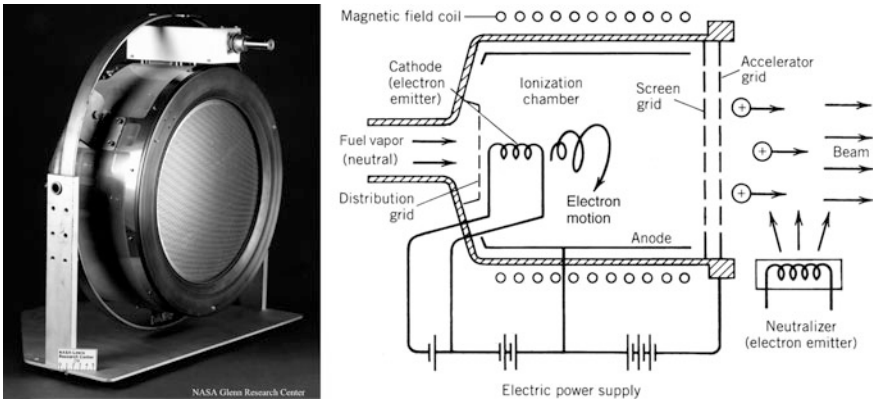

Fig. 5.1 The xenon-fueled NSTAR ion thruster of NASA's Glenn Research Center (left). *Credit* NASA/GRC. Schematic of an ion thruster (right). The electrostatic zone is between the screen grid (anode) and accelerator grid (cathode). *Credit* Sutton (2001), U. Walter

enter a very narrow electrostatic zone where they are accelerated in a high electric field. After emerging from this zone at an extremely high speed, typically 40 km s^{-1}, they are neutralized with the electrons separated earlier in the reaction chamber.

To begin with the physics of the acceleration mechanism, we define some essential quantities. Let Q be the total charge, q the charge density, N the number, n the number density, and ρ the mass density of the ions with unit charge e and mass m_{ion} in the thruster. Between these quantities and the ion beam current I_b the following basic relations hold:

$$\begin{array}{ll} Q = Ne & q = ne \\ \dot{Q} = \dot{N}e = I_b & \dot{q} = \dot{n}e \\ m_i = Nm_{ion} = m_{ion} \cdot Q/e & \rho = nm_{ion} = m_{ion} \cdot q/e \\ \dot{m}_i = \dot{N}m_{ion} = m_{ion} \cdot I_b/e & \dot{\rho} = \dot{n}m_{ion} = m_{ion} \cdot \dot{q}/e \end{array} \tag{5.2.1}$$

where m_i is the total ion mass. Now we turn to the key question: What is the thrust $F_* = \dot{m}_i v_*$ of such an ion thruster?

5.2.1 Ion Acceleration and Flow

The crucial component of the engine for thrust generation is the acceleration zone, which determines the required parameters $\dot{m}_p, v_e$. In order to derive them, we need to understand the charge distribution in the electrostatic zone between the two grids in detail (see Fig. 5.2). We assume the engine axis as the x-axis along which the ions are moving. They enter the zone through bores in the screen grid (anode) at $x = 0$. Then they are accelerated by an electric potential $V(x)$ (the form of which

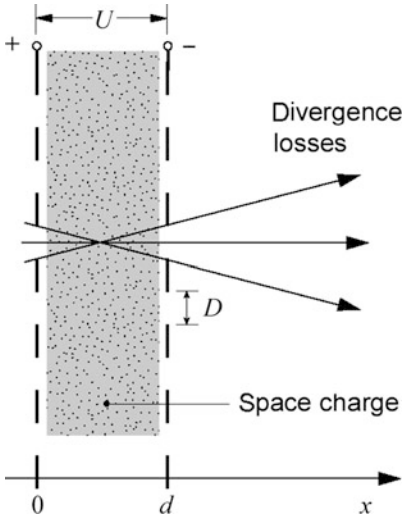

Fig. 5.2 Geometrical and electric relations in the electrostatic zone between the two grids

still has to be derived) between the screen grid (anode) and the accelerator grid (cathode) with separation d. The acceleration voltage across the grids is $U := V(d)$. Finally, the accelerated ions exit the zone through bores in the accelerator grid at $x = d$.

The charges flowing through this zone with velocity v generate a space charge with density q, which reduces the electric potential $V(x)$ so that the inflow of the charges is slightly reduced. The balance between charge and electric potential is physically described by the Poisson equation (cf. Eq. (7.1.1))

$$\frac{d^2V}{dx^2} = \frac{q(x)}{\varepsilon_0} \tag{5.2.2}$$

with ε_0 being the vacuum permittivity. Because of charge conservation along the whole acceleration distance $0 \leq x \leq d$, the resulting charge flow density $j = qv$ must be constant

$$j = qv = const \quad \textbf{charge continuity equation} \tag{5.2.3}$$

This is the equivalent equation to the mass continuity Eq. (1.2.8) for mass conservation. The particle velocity v at any place within the acceleration zone is determined by the balance between kinetic energy and electric potential energy, i.e.,

$$\frac{1}{2}m_{ion}v^2 = eV \tag{5.2.4}$$

with m_{ion} the mass of an ion, and e the charge of the singly charged ion, which is the elementary charge. At the end of the acceleration distance, the ejection velocity is determined from Eq. (5.2.4) and $U := V(d)$ as

$$v_e = \sqrt{\frac{2eU}{m_{ion}}} \tag{5.2.5}$$

For typical ion thrusters, we have $v_e = 30 - 80$ km s^{-1}. Therefore, ion thrusters are about one order of magnitude more efficient than chemical thrusters. Ion engines, however, share an important property with thermal engines (see Eq. (4.2.5)):

The efficiency of an ion thruster increases with decreasing molar mass of the propellant according to $I_{sp} \propto v_e \propto 1/\sqrt{M_p}$.

With Eq. (5.2.4), the charge density at any position in the zone can be determined through Eq. (5.2.3) as

$$q = j\sqrt{\frac{m_{ion}}{2eV}} \tag{5.2.6}$$

Inserting this expression into the master Eq. (5.2.2) for the electric potential V we obtain

$$\sqrt{V}\frac{d^2V}{dx^2} = \frac{j}{\varepsilon_0}\sqrt{\frac{m_{ion}}{2e}} =: c = const$$

To solve this differential equation we multiply both sides with $V' = dV/dx$ and get

$$V'V'' = cV'V^{-1/2}$$

Direct integration of both sides and taking the square root delivers $V' = 2\sqrt{c}V^{1/4}$ or

$$\frac{dV}{V^{1/4}} = 2\sqrt{c}\cdot dx$$

Integration of both sides and taking into account that $V(x = 0) = 0$ yields

$$V^{3/2} = \frac{9}{4}\frac{j}{\varepsilon_0}\sqrt{\frac{m_{ion}}{2e}}x^2 \tag{5.2.7}$$

This is the wanted electric potential function $V(x) \propto x^{4/3}$.

Remark *In case we would not have any charges in the electrostatic zone, Eq. (5.2.2) would read* $d^2V/dx^2 = 0$ *and hence the familiar* $V(x) \propto x$ *in vacuum would result. The weak modification of the linear electric potential function to a* $x^{4/3}$ *behavior is obviously caused by the space charge of the transiting ions.*

Charge and Mass Flow Densities

At location $x = d$ the acceleration potential is $V = U$ and we derive from Eq. (5.2.7) for the charge flow density at the exit

$$j_e = \frac{4\varepsilon_0}{9}\sqrt{\frac{2e}{m_{ion}}}\frac{U^{3/2}}{d^2} \quad \textbf{Child-Langmuir law} \tag{5.2.8}$$

Inserting this into Eq. (5.2.6), the charge density of singly charged ions at the exit is calculated with for $x = d$ and $V = U$ as

$$q_e = \frac{4}{9}\frac{\varepsilon_0 U}{d^2} \tag{5.2.9}$$

It is instructive to know the particle density at the exit n_e. This is easily derived from the relation $q = ne$ to be

$$n_e = \frac{4}{9}\frac{\varepsilon_0 U}{ed^2} \tag{5.2.10}$$

For typical values $U = 2\,000$ V and $d = 2$ mm we find $n_e = 1 \times 10^{10}$ cm^{-3}. For comparison, standard dry air has a particle density of $n_{air} = 5 \times 10^{19}$ cm^{-3} which equals about that at the exit of thermal engines at launch. The exhausted gas therefore has a density of about or more than nine orders of magnitude lower than thermal engines. The reason obviously is the strong charge repulsion of the ions in the acceleration zone. At such extremely low gas densities, the gas exit pressure is far below any atmospheric pressure. Operating it in an atmosphere would thus imply that the atmospheric gas would flow from outside into the ion chamber bringing the ionization to a stall. Therefore, ion thrusters only work in the vacuum of space.

The extremely low exhaust ion gas density also implies that the mass flow rate of an ion thruster is equally low. From Eq. (5.2.1) and from the continuity Eq. (1.2.8) applied to the exit we determine the ion mass flow rate $\dot{m}_i$ as

$$\dot{m}_i = \frac{m_{ion}}{e} I_b = \rho_e v_e A_e = \frac{4}{9}\sqrt{\frac{2m_{ion}}{e}}\frac{\varepsilon_0 A_e}{d^2} U^{3/2} \tag{5.2.11}$$

where I_b is the ion beam current. A typical value for today's ion thrusters with xenon fuel is $\dot{m}_i \approx 10^{-6}$ kg s^{-1}. Xenon is the most common propellant for ion thrusters, because it is naturally occurring (87ppb in atmosphere) and gaseous at ambient temperature. In addition it has a very low chemical reactivity, a low first ionization potential, high storage density, and a high atomic mass. The high atomic mass yields a better thrust-to-power ratio (see Eq. (5.2.22)).

5.2.2 *Ideal Engine Thrust*

With these results we are now able to determine the thrust of an ideal ion engine having $\bar{v}_e = v_e$, $\eta_{div} = 1$. To evaluate the relevance of the pressure thrust F_p we recall from Eq. (1.2.17) that $F_p/F_e \propto 1/v_e^2$. Because the ejection velocity for ion thrusters is with $v_e = 30 - 80$ km s^{-1} about one order of magnitude larger than for chemical engines, we establish that the pressure thrust is about two orders of

magnitude smaller than for chemical engines and hence negligible. The engine thrust in practical terms therefore is given solely by the momentum thrust as given by the general expression for jet engines in Eq. (1.2.16), $F_e = F_{ex} = \rho_e A_e v_e^2$, where ρ_e is the mass density at the exit of the engine with cross section A_e. Because from Eq. (5.2.1) $\rho = m_{ion} q/e$ and with Eq. (5.2.5) we can write for the momentum thrust

$$F_e = \rho_e A_e v_e^2 = 2 q_e A_e U \tag{5.2.12}$$

We now make use of Eq. (5.2.11) and insert Eq. (5.2.9) into Eq. (5.2.12) yielding

$$\begin{aligned} F_e &= \dot{m}_i v_e = \sqrt{\frac{2 m_{ion} U}{e}} I_b \\ &= 2 q_e A_e U = \frac{8}{9} \varepsilon_0 \left(\frac{U}{d}\right)^2 A_e \end{aligned} \tag{5.2.13}$$

Here U is the voltage applied across the acceleration grid and I_b the ion beam current. The exit surface A_e is the sum of all n bores with the diameter D in the cathode plate, i.e., $A_e = n\pi D^2/4$. Hence, thrust increases quadratically with the applied acceleration voltage and inversely proportionally to the square of the distance between the electrodes. So, the perfect ion thruster has the highest possible voltage with the smallest possible acceleration distance. A practical limit is reached when electrical flash-overs happen at about 10 kV mm^{-1}. For a typical xenon propellant we have $\sqrt{2 m_{Xe}/e} = 1.65$ mN A^{-1} V$^{-1/2}$ or $\sqrt{2e/m_{Xe}} = 1.21$ km s^{-1} V$^{-1/2}$. For common ion thruster parameters with $I_b = 1$ A, and $U = 1500$ V we typically get $F_e = 62$ mN and $v_e = 45$ km s^{-1}.

Comparison with Other Thrusters

With 10–200 mN the total thrust $F_* = \dot{m}_i v_*$ of an ion thruster is by several orders of magnitude smaller than that of chemical engines of comparable size. This alone wreckages its use as a launch engine. The reason is clear: Although the ejection velocity of ion thrusters is about ten times larger, the lack of momentum thrust is due to an extremely low mass flow rate, which, as already mentioned, in turn is due to the strong charge repulsion of the ions in the acceleration zone. So, taking into account the different particle masses for ion and chemical propellant, the mass flow rate for a chemical engine is about seven orders of magnitude larger than for an ion thruster at the same exit cross section (engine size). This finally results in a chemical engine with roughly 100,000 times more thrust than an ion thruster of similar size. These characteristics are summarized for the three most important engines for space propulsion in Table 5.2.

Table 5.2 Assessment of the figures of merit of three engine types in space propulsion

Engine type	$\dot{m}_p$	v_e (efficiency)	$F_* = \dot{m}_p v_e$ (thrust)
Chemical	++	O	++
Ion/Hall	− − −	+	− −
Nuclear	+	+	++

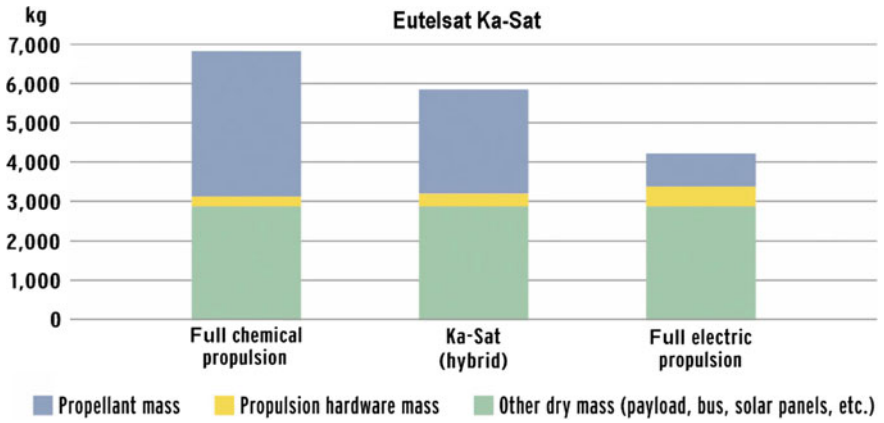

Fig. 5.3 The weight of Eutelsat's Ka-Sat in GEO at different propulsion designs. *Credit* Space News 2012

So, the nuclear (fission or even better fusion) engine would be an all-round engine if nuclear energy in space would not be banned by many societies today. This leaves us with only two distinct options: use massive chemical thrusters for launch and efficient ion thrusters for continuous in-flight orbit maneuvers or recurring station-keeping and attitude maneuvers. The promise of ion thrusters in the recurring maneuvers is depicted in Fig. 5.3 for the case of Eutelsat's Ka-Sat broadband communication satellite launched in December 2010 into GEO. With chemical thrusters for orbit-raising and ion thrusters for station keeping, i.e., with a hybrid design, it weighed 5900 kg. If it had used all chemical thrusters it would have weighed 6900 kg, too heavy for most commercial launchers. Using electric propulsion for orbit raising as well, Ka-Sat would have weighed no more than 4100 kg at launch, according to Eutelsat. At 2010's launch prices, going from a full-chemical to a all-electric propulsion design would have saved up to $60 million.

Nevertheless, for remote sensing satellites in LEO where propulsion mass for attitude-only maneuvers is not a key issue, small inexpensive chemical thrusters will still be more common than ion thrusters.

5.2.3 *Thruster Performance*

Thrust losses

Concerning thrust losses we have to take into account that ion thrusters exhibits jet divergences of typically $\alpha = 11 - 15^\circ$ yielding a divergence loss factor (see Sect. 1.2.1) of $\eta_{div} = (1 + \cos\alpha)/2 = 0.983 - 0.990$. In addition, it can be shown that the existence of multiply charged ions caused by multiple electron collisions in the discharge process causes thrust loss as expressed by a loss factor of typically $\eta_{++} = 0.98 - 0.99$. So, both make up an *exhaust loss factor* of

$$\eta_{ex} := \eta_{div}\eta_{++} = 0.96 - 0.98 \tag{5.2.14}$$

So by the same token as in Sect. 1.2.1. we have for the total thrust

$$\begin{aligned} v_* &= \eta_{ex}\, v_e \\ F_* &= \dot{m}_i v_* = \eta_{ex}\dot{m}_i\, v_e = \eta_{ex} F_e \end{aligned} \tag{5.2.15}$$

Note that at any time not all atoms in the discharge chamber are ionized. So, due to the chamber gas pressure some of the neutral atoms are leaking through the grids and are irreversibly lost. This neutral mass flow also contributes to the total propellant flow $\dot{m}_p$ but not to thrust.

Energy Conversion Loss

We recall from Sect. 1.3.3 that the *total engine efficiency*, which for an ion engine is the ratio of the jet power P_{jet} of the ion beam to the total electrical power into the thruster P_{in} is given as

$$\eta_{tot} = \zeta_d \zeta_v^2 \eta_{ec} \tag{5.2.16}$$

where in our case the energy conversion efficiency η_{ec} is

$$\eta_{ec} := \frac{P_{jet,id}}{P_{in}} = \frac{I_b U}{P_{in}} \tag{5.2.17}$$

The energy conversion efficiency tells us how much of the external electric power is transferred into the power of the beam. It therefore is a figure of merit for the quality of the engine.

For ion engines there are two prevailing energy conversion losses: discharge losses, i.e. power losses due to discharging electrons into the chamber that do not ionize atoms but hit the chamber anode unimpeded, and ionization losses due to the ionization of the ions. To see how these two come about, let E be energy, in particular E^+ the single ionization energy of an ion, P power, and N the number of ions with elementary charge e. Hence according to Eq. (1.3.14) and Eq. (5.2.1)

$$\begin{aligned} E_{jet} &= \frac{1}{2} m_i v_e^2 && \textbf{jet energy} \\ P_{jet,id} &= \frac{dE_{jet,id}}{dt} = \frac{1}{2}\dot{m}_i v_e^2 = I_b U && \textbf{jet power} \\ E_{jet,id} &= \frac{1}{2} m_i v_e^2 + NE^+ && \textbf{ionized-jet energy} \\ P^+_{jet,id} &= \frac{dE^+_{jet,id}}{dt} = \frac{1}{2}\dot{m}_i v_e^2 + \dot{N}E^+ = I_b(U + E^+/e) && \textbf{ionized-jet power} \end{aligned}$$

We consider these contributions by factorizing the energy conversion efficiency correspondingly

$$\eta_{ec} := \frac{P_{jet,id}}{P_{in}} = \frac{P_{jet,id}}{P^+_{jet,id}} \frac{P^+_{jet,id}}{P_{dis}} \cdot \ldots := \eta_+ \eta_{dis} \cdot \ldots = 0.55 - 0.75 \tag{5.2.18}$$

The figures given are derived from ion engines as given in literature. Discharge losses contribute (typically) by

$$\eta_{dis} \approx 0.86 \quad \textbf{discharge loss factor} \tag{5.2.19}$$

while ionization losses factor in as

$$\eta_+ := \frac{P_{jet,id}}{P^+_{jet,id}} = \frac{I_b U}{I_b (U + E^+/e)} = \frac{1}{1 + E^+/eU} \quad \textbf{ionization loss factor} \tag{5.2.20}$$

For xenon atoms with $E^+ = 12$ eV and typically $U = 1500$ V we find

$$\eta_+ = \frac{1}{1 + 0.008} = 0.99$$

Therefore while ionization losses are negligible, energy conversion is mostly limited by discharge losses.

Thrust-to-Power Ratio

With the above definitions we get from Eq. (5.2.16)

$$\eta_{tot} = \zeta_d \zeta_v^2 \eta_+ \eta_{dis} \cdot \ldots$$

In ion plasma there is no viscosity and no multiphase flow and hence $\zeta_d = 1$. Though there is velocity spread due to multiply charged ions, the correction factor ζ_v is negligible. Therefore

$$\eta_{tot} = \zeta_v^2 \eta_{ec} \approx \eta_{ec} = \eta_+ \eta_{dis} \cdot \ldots \tag{5.2.21}$$

Typical values for ion thrusters are $\eta_{tot} \approx \eta_{ec} = 0.55 - 0.75$.

We finally have from Eq. (1.3.23) and Eq. (5.2.5) for the important *thrust-to-total-power ratio*, which describes the thrust received from the total electrical power into the ion thruster,

$$\begin{aligned} r_{TTPR} &= \frac{F_*}{P_{in}} = \frac{2}{\bar{v}_e} \eta_{div}\, \eta_{VDF} \zeta_v^2 \eta_{ec} \\ &\approx \eta_{div}\, \eta_{VDF}\, \eta_{ec} \sqrt{\frac{2 m_{ion}}{eU}} \end{aligned} \quad \textbf{thrust-to-power ratio} \tag{5.2.22}$$

with

$$\eta_{div} \eta_{VDF} \eta_{ec} = 0.50 - 0.70$$

From this we learn that, though the ion thrust, $F_* \propto U^2$, increases with increasing acceleration voltage, the thrust-to-power ratio $r_{TTPR} \propto 1/\sqrt{U}$ decreases at the same time, yet at a much slower rate.

5.3 Electric Propulsion Optimization

Electric propulsion is special in that the ejection velocity and thus the specific impulse depends on the acceleration voltage and hence is variable. Due to the rocket Eq. (2.2.4) the propellant demand decreases exponentially with $v_* = g_0 I_{sp}$ (see Fig. 5.4). Would it then be feasible to get a steadily increasing payload ratio with an increasing acceleration voltage? This, unfortunately, is not the case, because with an increasing voltage also the mass of the power supply system increases which trades directly with payload mass. So, there exists an optimum I_{sp} where the total engine plus propellant mass of a spacecraft becomes minimal (see Fig. 5.4). We summarize this important fact by stating:

> The best ion engine for a mission with a given delta-v is NOT the one with the highest I_{sp}, but the one with that I_{sp} that minimizes the total engine mass.

In the following we want to derive means to determine an optimal S/C system layout. The following contributions add to the total mass of a S/C with an electric propulsion system

$$m_0 = m_p + m_s + m_L + m_g = m_p + m_f \tag{5.3.1}$$

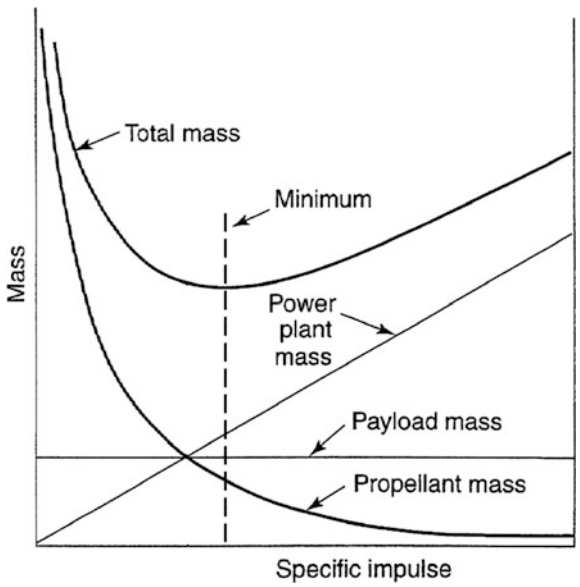

Fig. 5.4 The mass of a S/C with electrical engines has a minimum, as with increasing specific impulse the required propellant exponentially decreases, but the mass of the electric generator linearly increases

with m_s the structural mass, m_L the payload mass, and m_g the mass of the power plant. The latter can be, for instance, an RTG (radioisotope thermoelectric generator) or solar cells. If P_g is the electric power provided, then the so-called

$$\alpha := \frac{P_g}{m_g} \quad \textbf{specific power} \tag{5.3.2}$$

describes the mass-specific power output of the plant. Current plants are of order $100-200\ \mathrm{W\,kg^{-1}}$. The supplied power is converted into exhaust jet energy $\frac{1}{2}\dot{m}_p v_e^2$ (see Eq. (1.3.16)), at a given efficiency of the thruster η_t, i.e.

$$\frac{1}{2}\dot{m}_p v_e^2 = \frac{m_p}{2t_p} v_e^2 = \eta_t \alpha m_g \tag{5.3.3}$$

Here we have assumed a continuous mass flow over the total combustion time t_p. If we define the so-called

$$v_c := \sqrt{2\alpha t_p \eta_t} \quad \textbf{characteristic velocity} \tag{5.3.4}$$

we get the following relation between propellant mass and power plant mass

$$m_p = \frac{m_g}{\gamma^2} \tag{5.3.5}$$

with

$$\gamma := \frac{v_e}{v_c}$$

If we define

$$\mu := \frac{m_s + m_L}{m_0} \quad \textbf{payload ratio}$$

we find from Eqs. (5.3.1) and (5.3.5)

$$\mu = 1 - \frac{m_p}{m_0} - \frac{m_g}{m_0} = 1 - \frac{m_p}{m_0}\left(1+\gamma^2\right)$$

Because of Eq. (2.2.4)

$$e^{-\Delta v/v_e} = \frac{m_f}{m_0} = 1 - \frac{m_p}{m_0} \tag{5.3.6}$$

we get with the definition $\lambda := \Delta v / v_c$

$$\mu = e^{-\lambda/\gamma}\left(1+\gamma^2\right) - \gamma^2 \tag{5.3.7}$$

We now want to find the dependence of the propulsion demand (here λ) provided by the electrical engine on the variable ejection velocity and hence on γ at a given payload ratio μ. For this purpose we solve Eq. (5.3.7) with regard to λ and finally get

$$\lambda = \gamma \ln\left(\frac{1+\gamma^2}{\mu+\gamma^2}\right) \tag{5.3.8}$$

The curves $\lambda = \lambda(\gamma)$ with parameter μ are shown in Fig. 5.5. It is now our goal to find the maximum Δv provided by the engine at a given μ, where v_e is our variable. To find this maximum, we have to differentiate Eq. (5.3.8) and find its root. This leads to the following conditional equation for γ:

$$\ln\frac{1+\gamma^2}{\mu+\gamma^2} = \frac{2\gamma^2(1-\mu)}{(\mu+\gamma^2)(1+\gamma^2)} \tag{5.3.9}$$

Solving for γ gives the optimized $v_e/v_c = \gamma$ and via Eq. (5.3.8) the maximized $\Delta v/v_c = \lambda$ as a function of μ as shown in Fig. 5.6.

Having found the optimal parameters, the following calculation scheme can be given to optimize an electric propulsion system.

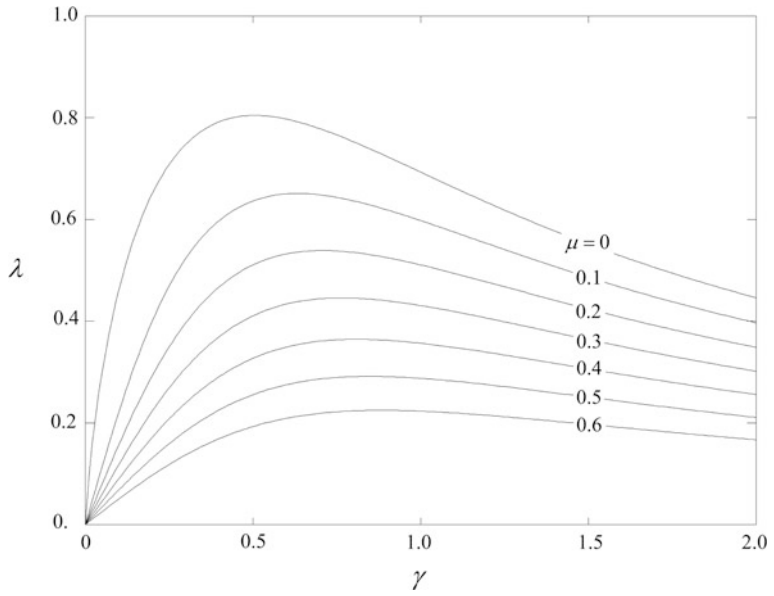

Fig. 5.5 The available normalized propulsion demand of an electric propulsion as a function of the normalized ejection velocity

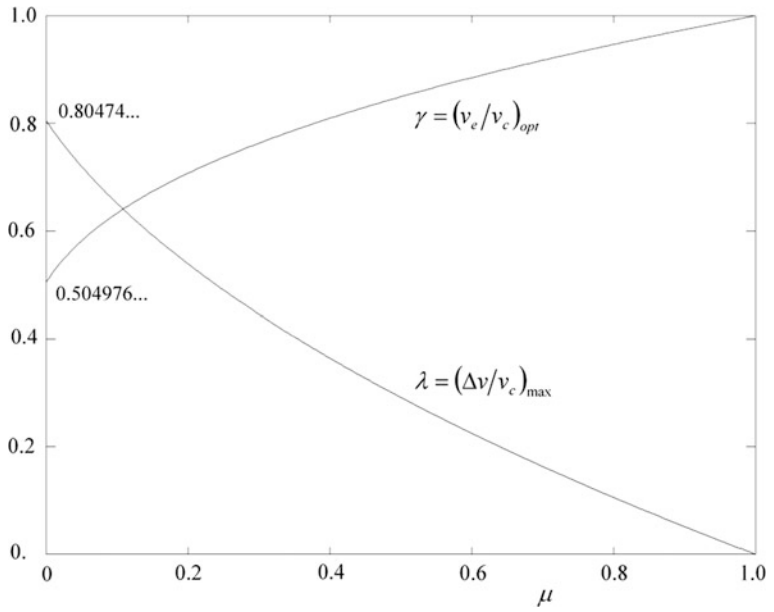

Fig. 5.6 The normalized optimal ejection velocity and the maximal available normalized propulsion demand of an electrical engine as a function of the payload μ

Calculation scheme

1. Determine from Eq. (5.3.9) or from Figure 5.6 for a given μ the optimal $\gamma = v_e/v_c$ and from Eq. (5.3.8) the corresponding maximized $\lambda = \Delta v/v_c$
2. Determine the propellant mass m_p from Eq. (5.3.6) and the power plant mass m_g from Eq. (5.3.5)
3. Determine at a given Δv the optimal v_e, or vice versa, through $v_e = \gamma \cdot \Delta v/\lambda$
4. Determine $v_c = v_e/\gamma$
5. For a given α and η_t determine the optimal burn time from $t_p = v_c^2/(2\alpha\eta_t)$.

As the payload mass is typically only a small percentage, approximate solutions can be provided for the limiting case $\mu \to 0$ (exercise, Problem 5.1)

$$\begin{aligned} \gamma &= 0.5050 \cdot (1 + 4.145\mu) \\ \lambda &= 0.8047 \cdot (1 - 2.461\mu) \\ m_p &= 0.7968 m_0 \, (1 - 2.685\mu) \\ m_g &= 0.2032 m_0 \, (1 + 5.606\mu) \\ v_e &= 0.6275 \cdot (1 + 6.606\mu)\Delta v \\ t_p &= 0.7721 \cdot (1 + 4.922\mu)\Delta v^2/\alpha\eta_t \end{aligned} \qquad @\ \mu < 0.04 \qquad (5.3.10)$$

Note *These are approximations in first order of* μ. *Therefore Eqs. (5.3.10) apply only as long as* $\mu \ll 1$. *It can be shown that for* $\mu < 0.04$ *the error* $\delta\gamma/\gamma$ *and with it also that of the other quantities remain below 5%.*

5.4 Problem

Problem 5.1 *Electric Engine Optimization (laborious)*
Prove that the linearized solution of Eq. (5.3.9) for $\mu \to 0$ are Eq. (5.3.10) by first showing with Newton's method that

$$\gamma = \gamma_0 \cdot \left[1 + \varepsilon\mu + O\left(\varepsilon^2\right)\right]$$
$$\gamma_0 = 0.504\,976\ldots$$

and

$$\varepsilon = \frac{\left(1+\gamma_0^2\right)^2}{2\gamma_0^2\left(1-\gamma_0^2\right)} = 4.145344\ldots$$